Design of a Multipipe, Counter-flow Heat Exchanger for Long-Distance and Commuter Buses

Name: Randy Balletta & Flannan Hehir
Date: May 5th, 2017

Executive Summary

In automobiles, nearly 70% of all fuel energy burned in an internal combustion engine is wasted via heat dissipated through the exhaust pipe, with only about a quarter of the fuel energy going towards vehicular motion. Recycling this wasted source of energy would improve the overall efficiency of the vehicle. For commuter bus vehicles that travel long distances daily, even a slight increase in the efficiency of the automotive energy system would lead to significant economic savings. Thus, the objectives of this report are as follows: (1) *design a heat exchanger concept to convert exhaust waste heat to electrical power by means of thermoelectric generators,* and (2) *establish the feasibility of the concept.*

After research and calculations, a multipipe, counter-flow heat exchanger using water as a coolant was developed. The design was corroborated by ample research, which pointed towards counter-flow heat exchangers because of their wide range of available operation temperatures. In addition, turbulent behavior and a large surface area were both desired to increase heat transfer, which was achieved or improved using three separate systems with thin pipes. In the design (Figure 1), an aluminum, square exhaust duct with fins lining the inside is surrounded by a layer of thermoelectric modules. Protecting the electronics from the coolant is an aluminum shell, a light metal with a high thermal conductivity. Finally, water, flows counter to the exhaust through a circular magnesium alloy pipe, a light but durable material used primarily to reduce weight.

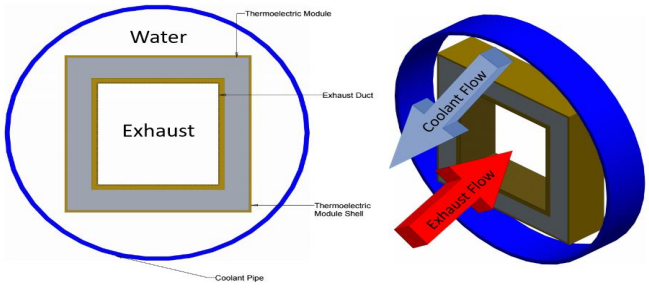

Figure 1: Cross-section view of pipe

The thermal analysis of the design was defined primarily by the modified Newton's law of cooling for both the exhaust and coolant pipes, in addition to the utilization of the Log Mean Temperature Difference (LMTD) method. These concepts relating the heat flow q were the basis for all subsequent analysis. Parametric studies were conducted to vary the outlet temperature of

the coolant $T_{c,o}$ and observe the end result behavior of performance parameters such as the overall heat exchanger length L and the total pump power P_{pump}. After also considering the effect of a figure of merit ξ, which considers design penalties of pump power and weight, and the L -P_{pump} tradeoff outlined by parametric studies, a value for $T_{c,o}$ was set to 618 °C. The overall performance of the design is summarized in Table 1.

When comparing the true power generation $\tilde{P}_{TE}$ to the total q in Table 1, it was determined that approximately 1% of the heat flow would be truly reused to generate electricity for the vehicle. Despite the small magnitude of this efficiency gain, there would still be economic incentive for a commuter bus company to use this heat exchanger design. When considering the fuel usage of the South Bend to Chicago route for a standard Coach USA bus, it was estimated that the specified heat exchanger could save one bus $3,500-3,700 per year, which would give a positive return on investment for the heat exchanger's manufacturing costs. While there is definitely room for improvement in areas such as fin design and thermoelectric generator efficiency, analysis of the design's performance assessed the heat exchanger as a beneficial addition to a commuter bus vehicle that could possibly be adapted to a wider range of vehicles types in the future.

Table 1. Summary of Final Design Performance and Critical Metrics (total values across all three heat exchanger pipes).

coolant mass flow rate $\dot{m}_c$ (kg/s)	**coolant inlet temperature $T_{c,i}$ (ºC)**	**coolant outlet temperature $T_{c,o}$ (ºC)**	**exhaust mass flow $\dot{m}_c$ rate (kg/s)**	**exhaust inlet temperature $T_{h,i}$ (ºC)**	**exhaust outlet temperature $T_{h,o}$ (ºC)**
0.0025	82.2	618	0.0219	704	82.8
thermoelectric power P_{TE} (W)	**coolant pump power $P_{pump,c,total}$ (W)**	**exhaust pump power $P_{pump,c,total}$ (W)**	**weight W (N)**	**figure of merit ξ**	**true thermoelectric power $\tilde{P}_{TE}$ (W)**
725.7	365.824	44.604	187.769	0.209	151.63

Detailed Design

Introduction:

Within in the automotive industry, approximately 70% of the heat energy produced by internal combustion engines is wasted [1]. Qualitatively understood, that means that about 18 quads (or, the equivalent energy needed to power 850 million suburban homes for a year) of the estimated 26.7 quads used in the transportation industry in the United States in 2012 were wasted, largely by means of heat dissipated via convection from exhaustion pipes [2]. Recently, automotive manufacturers have been closely exploring the practicality of thermoelectric modules in exhaust systems. Thermoelectric modules harvest energy by means of a temperature gradient between two surfaces, thereby outputting clean energy for immediate use or storage by the system from otherwise wasted heat. Good thermoelectric materials must boast the unique combination of a high electrical conductivity and low thermal conductivity, an uncommon amalgamation made easier to manufacture in large part due to improvements in nanotechnology. Nevertheless, expenditures and energy returns have kept thermoelectric modules off American roads.

The purpose of this design project was to design a heat exchanger for an automobile given initial specifications. More specifically, the objectives of the design were: (1) *design a heat exchanger concept to convert exhaust waste heat to electrical power;* and (2) *establish the feasibility of the concept*. After careful research into the design principles of heat exchangers and meticulous calculations to optimize the initial design, a multipipe, counter-flow heat exchanger using water as a coolant was developed. The resulting values of the system are tabulated in the summary table above (Table 1).

Design Constraints:

There were several design constraints. First, the thermoelectric module was assumed to have an efficiency of 5%. In addition, a single module had a mass m_{TE} of 10 g and was 27 x 27 x 5 mm in size, where the thickness t_{TE} was 5 mm. Second, the automobile was assumed to be at a steady highway speed v_{car} of 66 m.p.h., thereby discharging exhaust at a mass flow rate $\dot{m}_H$ of 21.9

g/s at an exhaust inlet temperature $T_{H,i}$ of 704 °C. Finally, the inlet temperature of the coolant $T_{C,i}$ was given to be 82.2 °C. Figure 1 depicts the counter-flow system of the heat exchanger. These specifications were used as the foundation of the design.

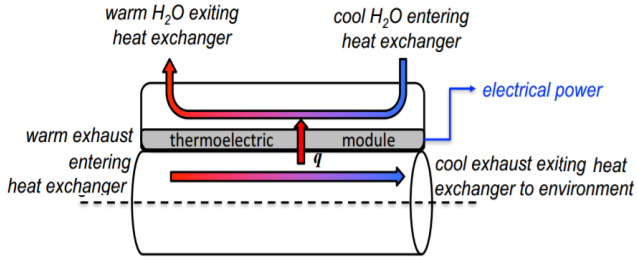

Figure 1: Schematic of counter-flow heat exchanger.

General Design:

Table 1 summarizes the final design performance and critical metrics for the system. That system is a multipipe, counter-flow heat exchanger, as depicted by the cross section in Figure 2. An aluminum square exhaust duct with fins lining the inside was surrounded by a layer of thermoelectric modules. Protecting the electronics from the coolant is an aluminum shell, a light metal with a high thermal conductivity. Finally, the coolant, water, flows through a circular magnesium alloy pipe, a light but durable material to reduce weight. Specific dimensions can be found in the part drawings (Appendix A). In addition, material properties and component lengths, volumes, and weights can be found in Appendix B (Table 1 and Table 2).

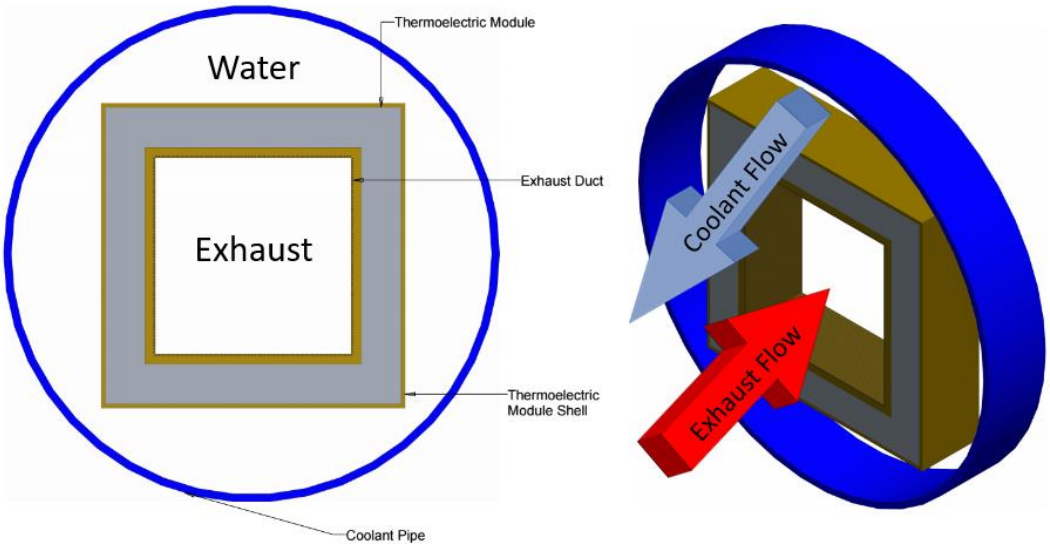

Figure 2: Cross-sectional schematic of counter-flow heat exchanger.

A counter-flow heat exchanger was selected based on its simplicity and the multitude of literature supporting its superior efficiency by virtue of the greater average temperature difference along any unit length than alternatives [3, 4, 5]. In addition, small diameters were chosen to induce turbulent flow, thereby increasing heat transfer. To increase surface area without sacrificing an improved heat transfer coefficient due to turbulence, the main exhaust flow was separated into three separate systems, each with their own heat exchanger (Figure 2). Fins were also added to the exhaust duct to similarly increase surface area.

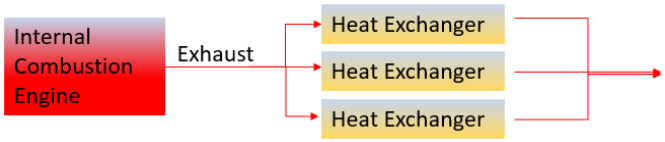

Figure 3: Schematic of the 3-pipe system. The "Heat Exchanger" piece includes the coolant counter flow, which is also sourced three separate pipes stemming from one.

To achieve a maximum temperature difference, the outlet temperature of the exhaust $T_{H,o}$ was set to 82.8 ^{o}C. After a parametric analysis (discussed later), the outlet temperature of the coolant $T_{C,o}$ was set to 618 ^{o}C. Fluid properties were measured at the averages of the inlet and outlet (Appendix B, Table 3). Though other options were explored such as dielectric fluids, water was selected as a coolant because of its availability and superior thermodynamic properties which produced good heat transfer coefficients. Materials for components were selected carefully to be simultaneously light and durable given driving conditions, and with little thermal resistances to inhibit heat transfer. As such, aluminum and a magnesium alloy, materials frequently seen in automotive parts, were selected, as they exhibit the desired behavior and are readily available from manufacturers (Appendix B, Tables 1 and 2) [7].

Initial Analysis Based on Design Constraints:

For ease of computation, this part of the study focuses on the calculation of design parameters for one of the three pipes, and the total values for all three pipes are outlined in the summary (Table 1). The analysis began with setting an outlet temperature for the exhaust pipe $T_{h,o}$ to a temperature slightly above the inlet temperature of the coolant, which allowed for the

maximum heat transfer from the exhaust to the coolant based on the design constraints. The Log Mean Temperature Difference (LMTD) method was utilized in conjunction with modified Newton's law of cooling for both fluid flows to formulate the following equations:

$$q = \dot{m}_c\, c_{p,c}(T_{c,o} - T_{c,i}) \,, \quad (1)$$

$$0.95q = \dot{m}_h\, c_{p,h}(T_{h,o} - T_{h,i}) \,, \quad (2)$$

$$q = R_{tot}\, \Delta T_{lm} \,, \quad (3)$$

where q is the total heat flow from the exhaust pipe to the coolant, $\dot{m}_h$ is the mass flow rate of the exhaust, $T_{c,o}$ is the outlet temperature for the coolant, $c_{p,c}$ and $c_{p,h}$ are the specific heat capacities for the coolant and exhaust (listed in Table X), R_{tot} is the equivalent thermal resistance of the heat exchanger, and ΔT_{lm} is the log mean temperature for a counter flow heat exchanger. The coefficient of q in Eq. (2) represents the heat flow that is transmitted to the coolant after 5% of the energy is channeled off by the thermoelectric modules. All of the values on the right hand side of Eq. (1) were known, thus q was calculated and listed in Table 1 as a constant value throughout the design.

After computing q, the remaining unknowns were $T_{c,o}$, $\dot{m}_c$, ΔT_{lm}, and R_{tot}, where ΔT_{lm} and $\dot{m}_c$ could be directly computed after setting a value for $T_{c,o}$ in Eqs. (1) and (3). The power distributed to the thermoelectric models P_{TE} was also computed by multiplying q by the given 5% efficiency of the modules, with the values of both q and P_{TE} stated in Table 1. Throughout the design process, a figure of merit ξ was used to assess the quality of the design and defined as,

$$\xi = P_{TE} - P_{pump} - P_W/P_{TE} \,, \quad (4)$$

where P_{pump} is the total power required to pump both the exhaust and coolant, and P_W is the power required to move the additional weight of the heat exchanger (Eq. (X), Appendix C).

Represented in Appendix C (Figure 1), a thermal resistance network was drawn for the designed heat exchanger. The following Eq. (4) for R_{tot} was defined as,

$$R_{tot} = R_{conv,h} + R_{cond,h} + R_{cond,TE} + R_{cond,shell} + R_{conv,c} \,, \quad (5)$$

where $R_{conv,h}$ is the convection resistance due to the air of the exhaust, $R_{cond,h}$ is the conduction resistance due to the aluminum exhaust pipe, $R_{cond,TE}$ is the conduction resistance of thermoelectric

material, $R_{cond,shell}$ is the conduction resistance of the TE module aluminum shell, and $R_{conv,c}$ is the convection resistance due to the water of the coolant pipe. The exact calculation of these resistance terms are detailed in Appendix C, Eqs. (2)-(4), with the only unknown variable being the length of the heat exchanger L in each equation's area term, and heat transfer coefficients for the exhaust and coolant, h_i and h_o, in Eqs. (2) and (4). Contact resistances and resistances due to fouling were deemed to be negligible to analysis, although likely present due to thin layers' epoxy adhesives in between materials and machining defects. Radiation was assumed to be negligible based on similar studies conducted for heat exchangers, but a more precise analysis involving computational fluid dynamics may benefit from including radiation terms in the thermal resistance network. Calculating the heat transfer coefficients involved finding the Reynold's number *Re* for pipe flow (Eq. (5), Appendix C), based on fluid properties at an average temperature between the inlet and outlet. For the purposes of parametric analysis, the Dittus-Boelter correlation Nusselt number *Nu* correlation for fully developed turbulent flow was used (Eq. (6), Appendix C), but more accurate correlations were used once optimal design values were selected.

Parametric Studies

By varying values for $T_{c,o}$ in a `MATLAB` script, ΔT_{lm}, $\dot{m}_c$, R_{tot}, and L could all be solved parametrically. Additionally, the pump power for each pipe could be defined generally as,

$$P_{pump,ind} = \Delta p \dot{m}/\rho \ , \qquad (6)$$

where $P_{pump,ind}$ is the power required to pump the coolant or exhaust for one of the individual pipes, Δp is the pressure drop across the pipe flow defined in Eq. (8) of Appendix C, and ρ is the density of either the exhaust or coolant. By using Eq.(2) and Eq. (7)-(8) of Appendix C, pump power equations for each of the exhaust and coolant pipes were derived and are shown in Appendix C (Eq. (9)-(10)). The total pump power P_{pump} for all three individual pipers of the heat exchanger was defined as,

$$P_{pump} = 3(P_{pump,c} + P_{pump,h}) \ . \qquad (7)$$

Combining Eqs. (3) and (5) and the resistance equations (Appendix C, Eqs. (2) through (5)) yielded a solution for L. Subsequently, the ΔT_{lm}, L, and P_{pump} were plotted as functions of $T_{c,o}$ in Appendix D (Fig. 1 and Fig. 2) to receive a general sense of their inner relationships. Since fluid dynamic properties could not be updated for each individual instance of $T_{c,o}$, the properties for the parametric plots were found at an average temperature of 550 ^{o}C [5].

Fig. 1 and Fig. 2 of Appendix D show that ΔT_{lm} decreases in a linear fashion with increasing $T_{c,o}$, L increases in a linear fashion with increasing $T_{c,o}$, and P_{pump} decreases exponentially with increasing $T_{c,o}$. To balance the trade-off of decreasing P_{pump} at the expense of decreasing L in addition to considering the value of ξ, a design value for $T_{c,o}$ of 618 ^{o}C was set. For the fluid properties in Table 3 (Appendix B), an average temperature between the inlet and outlet of 350 ^{o}C was used for water vapor, despite the initial phase of the water coolant being liquid.

Fin Analysis and Performance Comparison:

After comparing the contributions of the individual resistances of Eq. (5), it was determined that $R_{conv,h}$ was the dominant term. Consequently, the rectangular fins were applied to the inside of the exhaust pipes to effectively increase surface area and overall heat transfer. Eq. (2) in Appendix C was revised to the following:

$$R_{conv,h} = 1/\eta_0 h_i A_t \,, \qquad (8)$$

where η_0 is the overall fin efficiency found by using Eq. (2)-(4) of Appendix C, and A_t is the total fin surface area found by using Eq. (11)-(15) of Appendix C. After thorough iterations of different fin structures and geometries, it was determined that ξ was maximized using a large number of small, thin, rectangular fins in the exhaust pipes. The short-lengthened fins did not assume any central cross-sectional area of the pipe, which helped contribute to a higher η_0 value in comparison to designs with larger fins. Furthermore, the small volume assumed by the numerous fins aimed to preserve the turbulence of the exhaust flow. Unfortunately, later analysis proved that this would not be the case.

In *Re* calculations for the coolant flow, the water was deemed to be fully laminar at the set $T_{c,o}$ so a Nu = 3.66 for a constant temperature, laminar, cylindrical pipe flow was used. The *Re* for the exhaust flow was less than the critical value for turbulence onset of 4000, which was not what the design had intended for. The perimeter term in the denominator of *Re* Eq.(5) of Appendix C was heavily increased due to the added fin geometry, subsequently decreasing *Re*. Despite being an incorrect assumption, the Dittus-Boelter correlation for turbulent flow of a circular duct was still used for *Nu* of the exhaust because it represented a satisfactory design and empirical correlations of turbulent flows for square ducts were cumbersome to find. It should be noted that the duct geometry should be reanalyzed in future usage of this design for best heat reutilization performance.

Table 4 (Appendix B) lists the fin geometries and properties. After running through the analysis with and without fins, it was determined that the inclusion of fins decreased L by ~17% and increased ξ by a factor of 4 to a final value of 0.209. A summary of overall performance metrics can be found in Table 5 (Appendix B).

Feasibility:

By scaling the P_{TE} value by ξ, a true generation $\tilde{P}_{\mathrm{TE}}$ of 151.63 W was obtained, as seen in Table 5 (Appendix B). In comparison to the overall q calculated for the heat exchanger, only 1% of the heat flow is truly being reutilized to generate electricity for the vehicle. Because of the relatively miniscule gain from the design and manufacturing costs, this system cannot be recommended for small vehicles. Instead, this design would be ideal for larger highway vehicles traveling long distances. For example, a bus bound along the ninety-mile trek on Interstate 80 from South Bend, Indiana, to Chicago, Illinois, steaming along at approximately 66 mph saves 0.3 gallons of fuel per trip (assuming 3 mpg as per Coach USA website) with this design. With the average cost of gas in Illinois as $2.40, that is a savings of $0.72 per trip. At eight round trips a day for approximately 315 days a year, that is a net savings of about $3500 - $3700 a year. Most

importantly, this system would save even more money for longer trips, where the vehicle averages highway speeds for a long time. If the system is moving at a speed lower than typical highway traffic, the inlet temperature of the exhaust $T_{H,i}$ will be lower, therefore the temperature gradient between the exhaust and coolant would be not as significant. If the system is a moving faster than 66 mph, the inlet temperature of the exhaust $T_{H,i}$ will be higher, putting more strain on pumps and reaching some melting limits for materials if too high. However, long-distance buses rarely exceed 70 mph because of speed laws and the strain on engines. Thus, the maximum efficiency of this system is reached at steady highway speeds at approximately 66 mph.

Regarding manufacturing, most geometric dimensions were catered to meet industry standards for reasonable costs and widely available materials without the need of special nanomanufacturing. The coolant pipe material, a magnesium alloy, is cheap at $1.25 per pound, and easily bent into thin shapes [6]. Aluminum, used in the exhaust duct and the thermoelectric module's shell, is a cost-effective metal capable of withstanding the temperature difference and undergoing stress from motion. In addition, aluminum has been manufactured on the microscopic scale [7], so the tiny fins on the duct's inner surface are achievable (though that will increase cost). The length of the total unit (three separate heat exchangers) at 2.525 m, makes for easy application to the bottom of a commuter bus, which is around 10 m in length. The thermoelectric modules, however, would demand about $2244 because of the sheer number and complexity of them [8]. However, given the money saved by units with this system installed, the manufacturing and material costs are justifiably worth the price.

Improvement:

One of the biggest areas for improvement is achieving *Re* for exhaust flow that is sufficiently large enough for the fully turbulent flow assumption to be more accurate. Furthermore, the use of computational fluid dynamic programs such as ANSYS could provide more precise *Nu* correlations for the irregular geometries of the flow cross-sections created by finned and

rectangular exhaust duct. Additionally, the research and development of the thermoelectric modules could play an important role in the future enhancement of this design: the 5% efficiency of the thermoelectric is a value that has plenty of room for growth and could make the use of a heat reutilization heat exchanger more economically feasible for a wider range of vehicle types. Lastly, further research into materials science could yield more lightweight, thermal conductive materials to use for each component.

Conclusion:

As stated previously, this system would produce financial benefits and clean energy if installed on a typical commuter bus. The multi-pipe element of the design aimed to increase the overall surface area in the heat exchanger in addition to the fins on the inside of the exhaust ducts. This design considered parametric studies and the figure of merit ξ calculation to choose an optimal $T_{c,o}$ for the best overall performance, based on the design specifications given. Using a set $T_{c,o}$ of 618 ^{o}C and incorporating the fin structures defined in the CAD drawings of Appendix A and Table 4 of Appendix B, a final $\xi = 0.209$ was computed, which boaster a true generation $\tilde{P}_{TE}$ of 151.63 W of the 14.51 MW available. Based on practical perspectives of economic and manufacturing feasibility, this design offers significant benefits to private or public commuter bus companies, and could be possibly adapted to a wider range of vehicle types with future improvements.

References:

[1] Sniderman, D., June, 2012, "Using Waste Engine Heat in Automobile Engines," https://www.asme.org/engineering-topics/articles/automotive/using-waste-engine-heat-in-automobile-engines
[2] Lawrence Livermore National Laboratory, "Energy Flow Charts: Charting the Complex Relationships among Energy, Water, and Carbon," March 2002.
[3] Kee Robert J., 2011, "The design, fabrication, and evaluation of a ceramic counter-flow microchannel heat exchanger "et al. Applied Thermal Engineering. pp. 31.
[4] Kotrba, RON, October, 2016. "The Ins and Outs of Heat Exchangers," Biomass Magazine.
[5] Bergman, Theodore.L., Levine, Adrienne .S., Incropera, Frank .P, Dewitt, David P., 2011, Fundamentals of Heat and Mass Transfer, Wiley, Chap. 11, pp. 714-715.

[6] Lee, S., Ham, H.J., Kwon, January, 2013. “Thermal Conductivity of Magnesium Alloys in the Temperature Range from −125 °C to 400 °C,” S.Y. et al. Internal Journal of Thermophysics, pp. 34.
[7] A. Maity, T. C. Doan, J. Li, J. Y. Lin, H. X. Jiang. Realization of highly efficient hexagonal boron nitride neutron detectors. Applied Physics Letters, 2016; 109 (7)
[8] LeBlanc, S., Yee, Shannon K., Scullin, Mathew L., Dames, C., Goodson, Kenneth E., 2013. “Material and Manufacturing Cost Considerations for Thermoelectrics,” Elsevier. pp. 10-13.
[square duct resistance formula in appendix C source] Scott, Thomas. “Steady Heat Conduction, Chapter 3.” http://cecs.wright.edu/~sthomas/htchapter03.pdf

Appendix A:

The following appendix includes CAD drawings generated by Creo Parametric 3.0 for parts of the heat exchanger. More specifically, cross-sections of parts are illustrated, showing the dimensions of parts (but not the true length) and the material. The following drawings are included:

- Completed Assembly Cross-section
- Exhaust Duct
- Thermoelectric Module
- Thermoelectric Module Shell
- Coolant Pipe

Appendix B:

The following appendix includes a collection of tables mentioned in the text.

Table 1: Relevant material properties for parts.

Part	Material	Thermal Conductivity, k [W m^{-1} K^{-1}]	Thickness, t [mm]	Density, ρ [kg m^{-3}]	Melting Point, T_{melt} [^oC]
Exhaust Duct	Aluminum	212	1.0	2700	725
TE Module	Electronics	2.69	5.0	2743.5	N/A
TE Module Shell	Aluminum	212	0.5	2700	725
Coolant Pipe	Magnesium Alloy	84	1.0	1800	660

Table 2: Length, volume, and weight for parts.

Part	Length, L [m]	Volume, V [m^3]	Weight, W [N]
Exhaust Duct	2.5281	$7.878*10^{-4}$	20.869
Fins	2.5281	$8.687*10^{-5}$	2.3
Thermoelectric Module	2.5281	0.0048	130.5
TE Module Shell	2.5281	$5.682*10^{-4}$	15.05
Coolant Pipe	2.5281	0.00114	19.05

Table 3: Relevant fluid properties for exhaust (air) and coolant (water).

Fluid	Specific Heat, c_p [J kg^{-1} K^{-1}	Density, ρ [kg m^{-3}]	Prandtl Number, Pr	Thermal Conductivity, k [W m^{-1} K^{-1}]	Dynamic Viscosity, μ [N s m^{-2}]
Exhaust (Air)	1066.9	0.543	0.682	0.0495	$3.15*10^{-4}$
Coolant (Water)	10,100	575	.87	.668	$6.48*10^{-5}$

Table 4: Fin geometry for an indirviudal heat exchanger exhaust pipe.

Number of Fins, N	850
Fin Length, L_f	0.27 mm
Fin Thickness, t	0.1 mm
η_f	0.8736
η_0	0.8769
Total Area, A_t	0.559 m^2

Table 5: Overall performance value metrics in designs with and without fins.

	With Fins	**Without Fins**
$\boldsymbol{P_{TE}}$	725.7 W	725.7 W
$\boldsymbol{\xi}$	0.209	0.057
$\boldsymbol{\tilde{P}_{TE}}$	151.63 W	41.27 W
$\boldsymbol{L}$	2.525 m	3.03
Number of Thermoelectric modules used	1122	1346

Appendix C:

This appendix details equations referenced in the main text that were used in the design analysis process.

$\Delta T_{lm} = \Delta T_1 - \Delta T_2 / \ln(\Delta T_1 / \Delta T_2)$, (1)
with $\Delta T_1 = \Delta T_{h,i} - \Delta T_{c,o}$ and $\Delta T_2 = \Delta T_{h,o} - \Delta T_{c,i}$ for a counter-flow heat exchanger

$R_{conv,h} = 1/h_i A_i$, (2)
with h_i as the heat transfer coefficient of the air of the exhaust pipe, and A_i is the surface area of the inner exhaust pipe

$R_{cond} = 0.785 \ln(r_o/r_i)/2\pi Lk$ (3)
with r_o as the outer side length of the square duct, r_i as the inner side length of the square duct, k as the thermal conductivity of the material [source]

$R_{conv,c} = 1/h_o A_o$, (4)
with h_o as the heat transfer coefficient of the water of the coolant pipe, and A_o is the surface area of the water pipe

$Re = 4\dot{m}/P\mu$, (5)
with P being the perimeter of the cross-sectional area of the pipe flow, and μ being the dynamic viscosity of the fluid.

$Nu = 0.023 Re^{4/5} Pr^{0.3}$, (6)
Dittus-Boelter correlation for turbulent pipe flow of a circular duct

$\dot{m} = \rho u A_c$, (7)
with u being the mean velocity of the fluid flow, and A_c being the cross sectional area of the flow.

$\Delta p = f \rho u^2 \Delta x / 2D_h$, (8)
with f being the friction factor [for turbulent flow: $f = (0.79 \ln(Re_D) - 1.64)^{-2}$], Δx is the distance travelled down the pipe, and D_h is the hydraulic diameter, $4A_c/P$.

$P_{pump,c} = 0.2858\, f q^3 L / 2D_h c_{p,c} (\rho A_c)^2 (T_{c,o} - T_{c,i})^3$ (9)

$P_{pump,h} = f \dot{m}_h u^2 L / 4D_h$ (10)
where D_h equals the side length of the inner square duct (0.025 m), and u can be computed directly from (7).

$A_f = 2L_f L$, (11)
where A_f is the surface area of a single rectangular fin, and L_f is the length of the fin from the base.

$A_t = A_b + NA_f$, (12)
where A_t is the total surface area of the inside of the exhaust pipe, A_b is the area of the exposed base on the inside of the exhaust duct, and N is the number of fins.

$$m = \sqrt{\frac{h_i P}{k A_c}} \quad (13)$$

where m is a parameter used in the calculation of η_f, defined in Eq. (13).

$$\eta_f = \tanh(mL_f)/mL_f \,, \quad (14)$$

where η_f is the fin efficiency.

$$\eta_0 = 1 - NA_f (1 - \eta_f) / A_t \,, \quad (15)$$

where η_0 is the overall fin efficiency for the total number of fins.

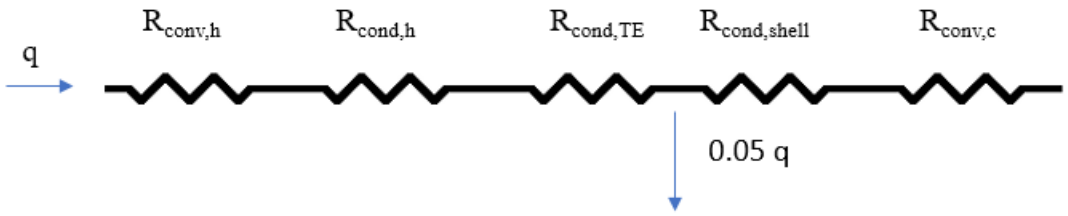

Figure 1: Thermal resistance network of system.

Appendix D:

This appendix includes figures referece in the main text.

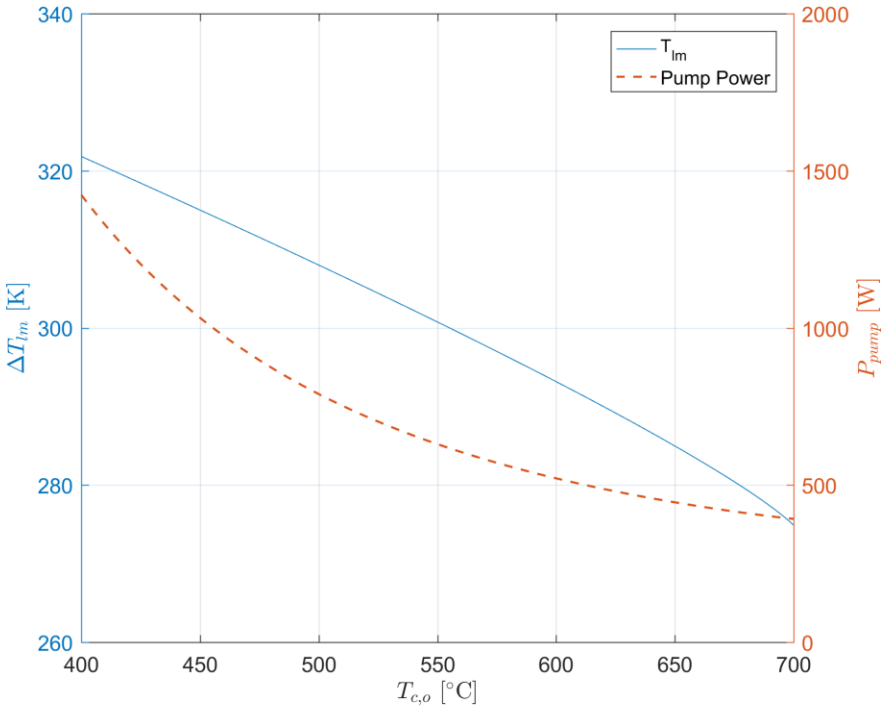

Figure 1. MATLAB plot of ΔT_{lm} and P_{pump} as a function of $T_{c,o}$.

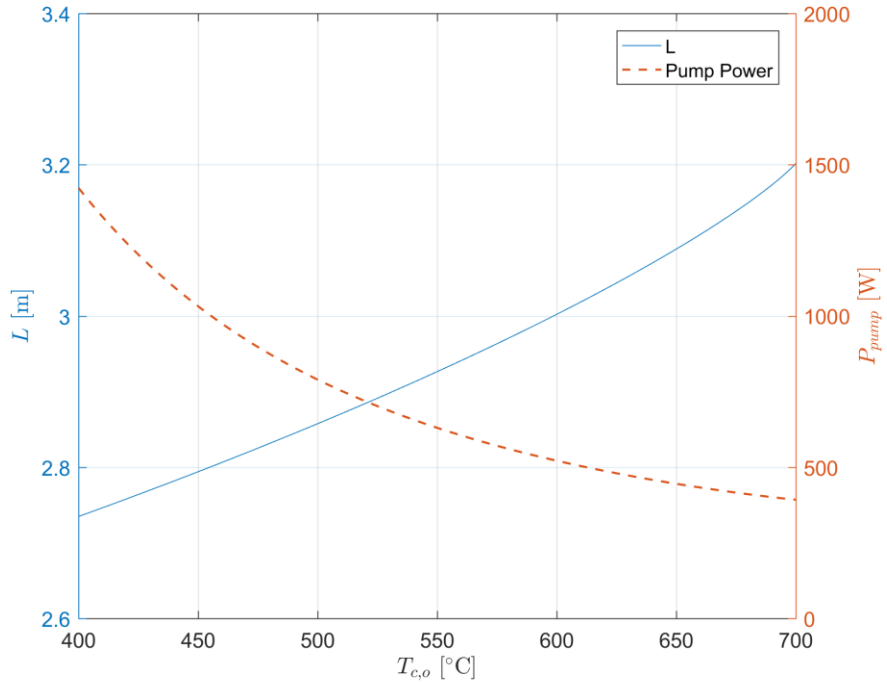

Figure 2. MATLAB plot of L and P_{pump} as a function of $T_{c,o}$.